International Journal of Innovative Computing, Information and Control
Volume **7**, Number **7(B)**, July **2011**

ICIC International ©2011 ISSN 1349-4198
pp. **4423–4434**

ADAPTIVE CONTROL METHOD FOR PATH-TRACKING CONTROL OF AN OMNI-DIRECTIONAL WALKER COMPENSATING FOR CENTER-OF-GRAVITY SHIFTS AND LOAD CHANGES

Renpeng Tan[1], Shuoyu Wang[1], Yinlai Jiang[1], Kenji Ishida[2]
Masakatsu G. Fujie[3] and Masanori Nagano[4]

[1]School of Systems Engineering
Kochi University of Technology
No. 185, Miyanokuchi, Tosayamada, Kami, Kochi 782-8502, Japan
138003t@gs.kochi-tech.ac.jp; { wang.shuoyu; jiang.yinlai }@kochi-tech.ac.jp

[2]Department of Physical Medicine and Rehabilitation
Kochi University
2-5-1 Akebono-cho, Kochi 780-8520, Japan
ishidake@kochi-u.ac.jp

[3]Department of Modern Mechanical Engineering
Waseda University
59-309, 3-4-1 Okubo, Shinjyuku, Tokyo 169-8555, Japan
mgfujie@waseda.jp

[4]Soai Co., Ltd.
266-2 Shigekura, Kochi, Kochi 780-0002, Japan

Received June 2010; revised October 2010

Abstract. *In previous studies, an omni-directional walker was developed for walking rehabilitation. Walking training programs are stored in the walker so that rehabilitation can be carried out without a physical therapist. However, the walker sometimes strays from the predefined path because of center-of-gravity shifts and load changes. It is necessary for the walker to precisely follow the paths defined in the walking training programs to guarantee the effectiveness of rehabilitation and user safety. Therefore, this paper describes a path-tracking control method for the omni-directional walker to compensate for center-of-gravity shifts and load changes. First, the kinematics and kinetics of the omni-directional walker motion are presented. Second, an adaptive control strategy is proposed. Finally, simulations show that the walker can be controlled accurately by using the proposed method.*

Keywords: Omni-directional walker, Adaptive control, Load change, Center-of-gravity shift, Path tracking

1. **Introduction.** In an aging society with a low birthrate, such as that found in Japan, an increasing number of people suffer from walking impairments due to illness or accident. Therefore, the demand for walking rehabilitation has been increasing in recent years. However, Japan has a serious shortage of physical therapists. Therefore, developing a walking training machine that can efficiently conduct a variety of training programs is highly desirable.

Walking is a complex combination of motions [1], which includes not only forward and backward motions, but also right and left motions, oblique motions and rotations. Thus far, walkers for walking rehabilitation have only allowed a few basic motions with the help of crutches, canes, and parallel bars. This holds true for lift walkers [2], active walkers [3], the SRC walker (Arizono Orthopedic Supplies Co., Japan) and the posture control walker

(Pacific Supply Co., Japan). The whole process of rehabilitation using these walkers requires the assistance of physical therapists, which is a heavy burden on the therapists, both mentally and physically. If a walker training machine for rehabilitation that does not require direct assistance of a therapist and that accommodates these diverse motion groups can be designed, then faster recoveries can be achieved and the burden on physical therapists will be reduced.

In previous studies, the authors of the present paper, along with colleagues, developed an omni-directional walker [4]. This walker allows omni-directional movement. Training programs are stored in the walker so that rehabilitation can be carried out without the presence of physical therapists. Its effectiveness in walking rehabilitation was verified by clinical tests [5-7]. However, the accuracy of the path tracking of this walker needed to be improved to make it possible for the walker to follow precisely the exercise programs prescribed by physical therapists. This paper focuses on the accuracy of path tracking for a nonlinear system taking into consideration center-of-gravity shifts and load changes caused by the users.

Optimal control [8,9] can achieve an optimal value of an evaluation indicator, but the value of the plant parameters needs to be known for the design of the controller. Although PID control [10] does not require the exact values of the plant parameters, because the optimal value of the PID control parameters can be obtained by iterative adjustment, the parameters of the controller need to be re-adjusted once the plant parameters change. Adaptive control [11,12] does not need the exact values of the plant parameters and can adapt to parameter uncertainties by measuring and adjusting the parameters automatically. Therefore, when the parameters are variable, adaptive control is more suitable. In the case of the omni-directional walker, the center-of-gravity shifts and load changes caused by the users during walking training introduce the parameter variability. Linear model reference adaptive control cannot be applied to the omni-directional walker, which is a nonlinear system. Inspired by Slotine and Li [13], we have now developed an original control method for the omni-directional walker.

In this paper, an adaptive control strategy is proposed for the omni-directional walker, which is a slowly time-varying nonlinear system. For a walker with parametric, structural, and environmental uncertainties, the proposed adaptive control provides adaptation mechanisms that adjust a controller to achieve the desired system performance. This paper is organized as follows: Section 2 describes the design of the structure, the kinematics, and the kinetics analysis of the omni-directional walker; Section 3 presents an adaptive control strategy to adapt to the center-of-gravity shifts and load changes caused by users during rehabilitation; Section 4 shows simulations of the proposed method with center-of-gravity shifts and load changes; the simulation results show that the proposed adaptive control method is feasible and effective; a brief conclusion is given in Section 5.

2. **Structure of the Omni-directional Walker and Modeling.**

2.1. **Omni-directional walker.** The structure of the omni-directional walker is shown in Figure 1. The most important feature of the walker is the use of omni-directional wheels. An arrangement of four omni-wheels at the bottom of the walker body enables the walker to move in any direction while maintaining its orientation.

The physical parameters of the omni-directional walker are listed in Table 1. Two telescopic poles are designed to support both the upper part of the walker and the load from the user. The walker height is adjustable from 900 to 1200 mm to accommodate the different heights of the users. The mass of the walker is 58 kg and the maximum speed is set to 0.25 m/s to ensure user safety.

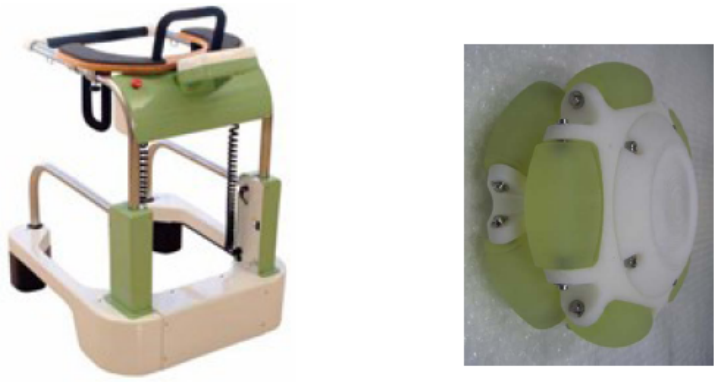

FIGURE 1. Omni-directional walker and one of its omni wheel

TABLE 1. Physical parameters of the walker

Parameter	*Value*
Height	*900 – 1200 mm*
Arm L	*400 mm*
Mass M	*58 kg*
Maximum load m	*80 kg*
Maximum speed v	*0.25 m/s*

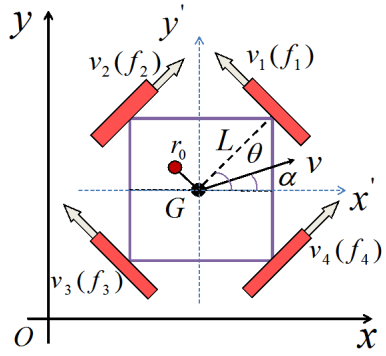

FIGURE 2. Structural model of the omni-directional walker

2.2. **Motion modeling.** To develop the control law for the omni-directional walker, we derive the necessary kinematic and kinetic equations. The coordinate settings and structural model are shown in Figure 2.

The parameters and coordinate system are as follows:

$\sum(x, y, O)$: Absolute coordinate system.

$\sum(x', y', G)$: Translation coordinate system of $\sum(x, y, O)$.

v: Speed of the omni-directional walker.

v_i: Speed of an omni-directional wheels $(i = 1, 2, 3, 4)$.

f_i: Force on each omni-directional wheel.

L : Distance from the center-of-gravity of the walker to each omni-wheel.

α: Angle between the x'-axis and the direction of v.

θ: Angle between the x'-axis and the position of the first omni-directional wheel.

G: Center-of-gravity of the walker.

r_0: Distance between G and the center-of-gravity caused by load.

Using the coordinate system shown in Figure 2, a kinematic analysis is carried out for the four-input, three-output nonlinear system. The kinematic equations are

$$\begin{cases} v_1 = -v_x \sin\theta + v_y \sin\left(\frac{\pi}{2} - \theta\right) + L\dot{\theta} \\ v_2 = v_x \cos\theta + v_y \cos\left(\frac{\pi}{2} - \theta\right) - L\dot{\theta} \\ v_3 = -v_x \sin\theta + v_y \sin\left(\frac{\pi}{2} - \theta\right) - L\dot{\theta} \\ v_4 = v_x \cos\theta + v_y \cos\left(\frac{\pi}{2} - \theta\right) + L\dot{\theta} \end{cases} \tag{1}$$

where $v_x = v\cos\alpha$ and $v_y = v\sin\alpha$ are the x and y components of the walker's velocity, respectively.

The linear relations in (1) imply

$$v_1 + v_2 = v_3 + v_4 \tag{2}$$

Equation (2) demonstrates that the velocity of each wheel of the omni-directional walker is restrained by those of the other three wheels.

The kinetic equations are the following:

$$\begin{cases} (M+m)\ddot{x}_G = -f_1 \cos\left(\frac{\pi}{2} - \theta\right) + f_2 \cos\theta - f_3 \cos\left(\frac{\pi}{2} - \theta\right) + f_4 \cos\theta \\ (M+m)\ddot{y}_G = f_1 \sin\left(\frac{\pi}{2} - \theta\right) + f_2 \sin\theta + f_3 \sin\left(\frac{\pi}{2} - \theta\right) + f_4 \sin\theta \\ (I + mr_0^2)\ddot{\theta} = Lf_1 - Lf_2 - Lf_3 + Lf_4 \end{cases} \tag{3}$$

where M is the mass of the omni-directional walker; m is the equivalent mass that the user imposes on the omni-directional walker, which varies according to the user's weight and walking disability; and I is the inertia of mass.

In this paper, the simulation model for the omni-directional walker is based on (3). As can be seen from this system of differential equations, the system is nonlinear because direction angle θ changes over time. Although there are four forces to control, f_1, f_2, f_3 and f_4, only three of these are independent because of linear relation (2).

3. Control Design.

In this section, we develop a motion control method for the omni-directional walker based on adaptive control theory. We can summarize the kinetic Equations (3) in matrix form:

$$M_0\ddot{X} = BF \tag{4}$$

where M_0, B, $\ddot{X}$ and F are defined as:

$$B = \begin{bmatrix} -\sin\theta & \cos\theta & -\sin\theta & \cos\theta \\ \cos\theta & \sin\theta & \cos\theta & \sin\theta \\ L & -L & -L & L \end{bmatrix}$$

$$M_0 = \begin{bmatrix} M+m & 0 & 0 \\ 0 & M+m & 0 \\ 0 & 0 & I + mr_0^2 \end{bmatrix}$$

$$F = \begin{bmatrix} f_1 & f_2 & f_3 & f_4 \end{bmatrix}^T$$

$$\ddot{X} = \begin{bmatrix} \ddot{x}_G & \ddot{y}_G & \ddot{\theta} \end{bmatrix}^T$$

Theorem 3.1. *Consider the nonlinear system (4) with control*

$$F = B^T \left(BB^T\right)^{-1} \left[\hat{M}_0 \left(\ddot{X}_d + \lambda\dot{e}\right) + KS\right] \tag{5}$$

and adaptive law

$$\dot{\hat{\alpha}} = \Gamma^{-1} HS \tag{6}$$

where

$$H = \begin{bmatrix} \ddot{x}_{Gd} + \lambda_1 \dot{e}_1 & 0 & 0 \\ 0 & \ddot{y}_{Gd} + \lambda_2 \dot{e}_2 & 0 \\ 0 & 0 & \ddot{\theta}_d + \lambda_3 \dot{e}_3 \end{bmatrix}$$

$$\hat{M}_0 = \begin{bmatrix} \hat{M} + \hat{m} & 0 & 0 \\ 0 & \hat{M} + \hat{m} & 0 \\ 0 & 0 & \hat{I} + \hat{m}\hat{r}_0^2 \end{bmatrix}$$

$X_d = [x_{Gd}, y_{Gd}, \theta_d]^T$

$X = [x_G, y_G, \theta]^T$

$e = X_d - X$

$S = \dot{e} + \lambda e$

and the parameters of adaptive control are

$$\lambda = \begin{bmatrix} \lambda_1 & 0 & 0 \\ 0 & \lambda_2 & 0 \\ 0 & 0 & \lambda_3 \end{bmatrix} \quad K = \begin{bmatrix} k_1 & 0 & 0 \\ 0 & k_2 & 0 \\ 0 & 0 & k_3 \end{bmatrix} \quad \Gamma = \begin{bmatrix} \Gamma_1 & 0 & 0 \\ 0 & \Gamma_2 & 0 \\ 0 & 0 & \Gamma_3 \end{bmatrix}$$

Then, error e converges as time $t \to \infty$, and all signals in the closed-loop system are bounded.

Proof: Control model Equation (4) is rewritten to derive the estimation formula [13].

$$\hat{M}_0 \ddot{X} = Y \hat{\alpha} \tag{7}$$

where $\hat{M}_0$ is an estimate of M_0, Y is defined by

$$Y = \begin{bmatrix} \ddot{x}_G & 0 & 0 \\ 0 & \ddot{y}_G & 0 \\ 0 & 0 & \ddot{\theta} \end{bmatrix}$$

and $\hat{\alpha}$ is an estimate of the diagonal elements of M_0, which is represented as follows: $\hat{\alpha} = \begin{bmatrix} \alpha_0 & \alpha_1 & \alpha_2 \end{bmatrix}^T$, $\alpha_0 = \hat{M} + \hat{m}$, $\alpha_1 = \hat{M} + \hat{m}$, $\alpha_2 = \hat{I} + \hat{m}\hat{r}_0^2$.

In order to analyze the closed-loop system stability, the Lyapunov-like function candidate is specified as:

$$V = \frac{1}{2}\left[S^T M_0 S + \Delta^T \alpha \Gamma \Delta \alpha\right] \tag{8}$$

where estimation error $\Delta\alpha$ is generated as $\Delta\alpha \triangleq \hat{\alpha} - \alpha$.

Differentiating (8) with respect to time and substituting using (5) and (6) yields:

$$\begin{aligned} \dot{V} &= S^T M_0 \dot{S} + \frac{1}{2} S^T \dot{M}_0 S + \Delta^T \alpha \Gamma \Delta \dot{\alpha} \\ &= S^T M_0 \left[\left(\ddot{X}_d - \ddot{X}\right) + \lambda\left(\dot{X}_d - \dot{X}\right)\right] + \Delta^T \alpha \Gamma \dot{\hat{\alpha}} \\ &= -S^T \left\{M_0 \ddot{X} - M_0 \left[\ddot{X}_d + \lambda(\dot{X}_d - \dot{X})\right]\right\} + \Delta^T \alpha \Gamma \dot{\hat{\alpha}} \\ &= -S^T K S - S^T \left(\hat{M}_0 - M_0\right)\left[\ddot{X}_d + \lambda(\dot{X}_d - \dot{X})\right] + +\Delta^T \alpha \Gamma \dot{\hat{\alpha}} \\ &= -S^T K S \leq 0 \end{aligned} \tag{9}$$

where the $\frac{1}{2} S^T \dot{M}_0 S$ term drops out because we assume M_0 is a constant matrix.

In (8), V is positive definite from the positive-definiteness of matrices M_0 and Γ. Hence, V plays the role of a Lyapunov function. Although (9) alone only shows that the time derivative of V is non-positive definite, $\dot{V} = 0$ would imply $S = 0$, which, from $S = \dot{e} + \lambda e$, would imply $\dot{e} = 0$ and $e = 0$. Since all the signals in the closed-loop system are bounded and e converges to zero as $t \to \infty$, the designed system is stable.

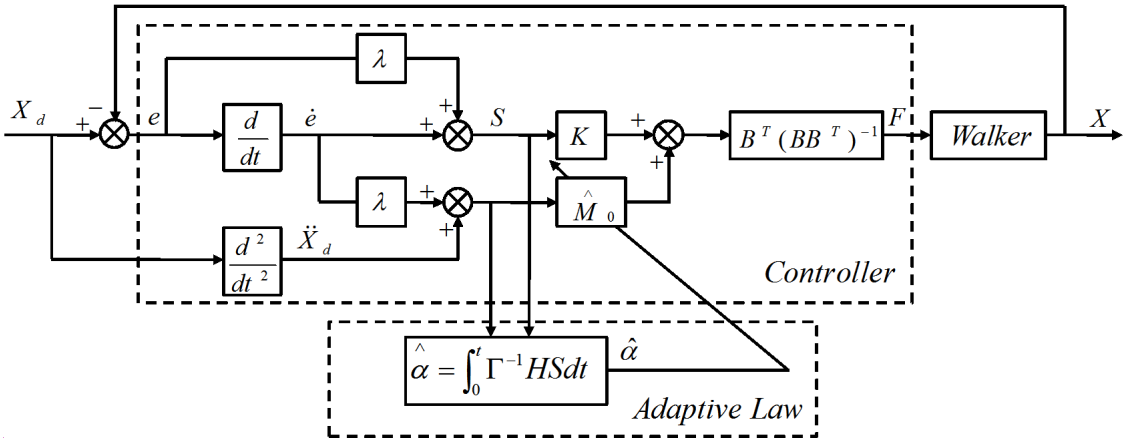

FIGURE 3. Block diagram of the adaptive control system

Figure 3 shows a block diagram of the control system presented in Theorem 3.1. The adaptive estimation parameter $\hat{\alpha}$ obeying adaptive law (6) updates the control law to control the walker.

Remark 3.1. *It should be noted that the result in Theorem 3.1 is based on the assumption that both M_0 is a constant matrix and the system is only slowly time-varying.*

4. **Simulation.** According to the rehabilitation plans designed by physical therapists, the omni-directional walker needs to realize several kinds of movement mainly composed of sequences of linear and rotational movement. Therefore, two simulations to verify the proposed control algorithm are presented in this section. One simulation is of controlling the walker to follow a linear path, and the other is of controlling the walker to follow a circular path.

4.1. **Simulation setting.** The physical parameters of the omni-directional walker used in the simulation are listed in Table 1.

The path to be followed is described by

$$y_{Gd} = x_{Gd} \tag{10}$$

Because the initial and final velocities are zero in real walking rehabilitation, we used these same values in our simulation trajectory. The trajectory is described by

$$\begin{aligned} x_{Gd}(t) &= d(t) + a \\ y_{Gd}(t) &= d(t) + a \\ \theta_d(t) &= \frac{\pi}{2} \end{aligned} \tag{11}$$

where

$$d(t) = \begin{cases} \frac{At}{2} - \frac{AT}{8\pi} \sin\left(\frac{4\pi t}{T}\right) & \left(0 \le t < \frac{T}{4}\right) \\ -\frac{AT}{8} + At & \left(\frac{T}{4} \le t < t_0\right) \\ -\frac{AT}{8} + \frac{A(t+t_0)}{2} - \frac{AT}{8\pi} \sin\left(\frac{4\pi}{T}\left(t - t_0 + \frac{T}{4}\right)\right) & \left(t_0 \le t < t_0 + \frac{T}{4}\right) \end{cases}$$

The physical therapists can change the parameter t_0 according to the requirements of individual users undergoing rehabilitation. The orientation angle is constant in the case of a linear path. Where $A = 0.2$ m/s, $a = 2$ m.

In the case of a circular path, a time-variant orientation angle is used. The path to be followed is described by

$$(x_{Gd} - x_0)^2 + (y_{Gd} - y_0)^2 = r^2 \tag{12}$$

where x_0 and y_0 specify the center of the circle, and r is the radius. In the simulation, values $x_0 = 4$ m, $y_0 = 4$ m and $r = 3$ m are used. As with the linear path, both initial and final velocities are chosen to be zero. The trajectory is described by

$$\begin{aligned} x_{Gd}(t) &= x_0 + r \cdot \cos\left[\frac{1}{r} \cdot \left(\frac{a_1}{3}t^3 + \frac{b_1}{2}t^2\right)\right] \\ y_{Gd}(t) &= y_0 + r \cdot \sin\left[\frac{1}{r} \cdot \left(\frac{a_1}{3}t^3 + \frac{b_1}{2}t^2\right)\right] \\ \theta_d(t) &= \frac{2\pi \cdot t}{142} + \frac{\pi}{2} \end{aligned} \tag{13}$$

where $a_1 = -3.93 \times 10^{-5}$ rad·m/s^3 and $b_1 = 5.61 \times 10^{-3}$ rad·m/s^2. The parameters a_1 and b_1 can be changed by physical therapists according to the individual requirements of the user undergoing rehabilitation.

We simulate the proposed adaptive control algorithm using the kinetics model (3) with different loads and center-of-gravity shifts. The same parameters (λ, K and Γ) for the adaptive controller are applied and adjusted for the case $m = 0$ kg and $r_0 = 0.00$ m in the following simulations.

4.2. **Simulation results.** Figure 4 and Figure 5 show simulations of the proposed adaptive controller being applied to the tracking of a linear path with initial position $x_G(0) = 1$ m, $y_G(0) = 1$ m, and $\theta(0) = 0.75\pi$ rad using the trajectory described in Equation (11). Figure 4 and Figure 5 show simulations for $m = 0$ kg and $r_0 = 0.00$, and $m = 50$ kg and $r_0 = 0.20$ m, respectively. In Figures 4(a), 4(b), 5(a) and 5(b), the horizontal axes indicate

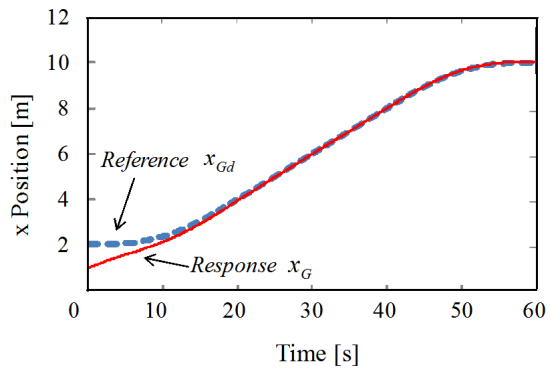

(a) Tracking performance for x position

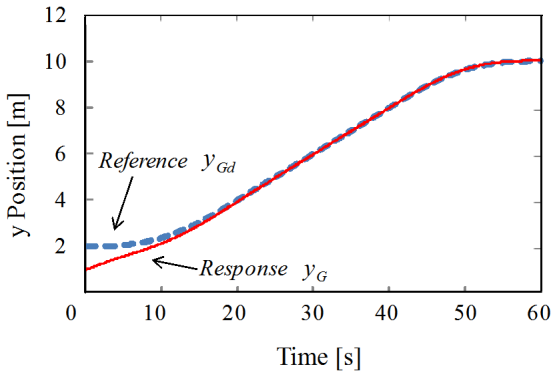

(b) Tracking performance for y position

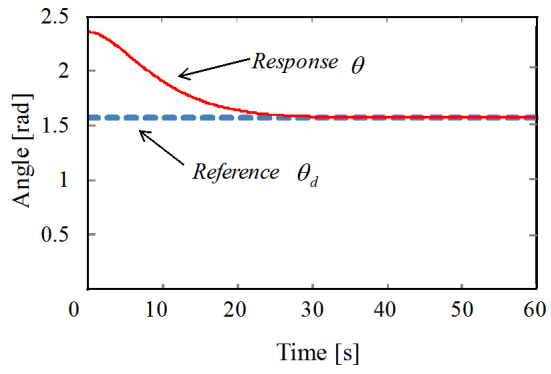

(c) Tracking performance for orientation angle θ

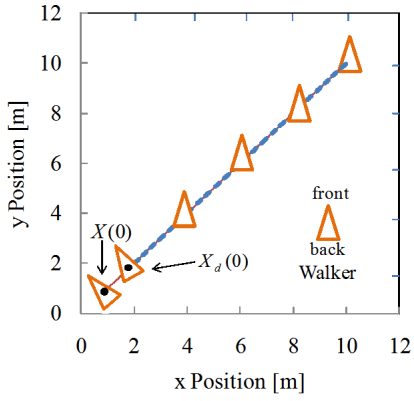

(d) Tracking and gradient of the walker

FIGURE 4. Simulation results for linear path with $m = 0$ kg and $r_0 = 0.00$ m

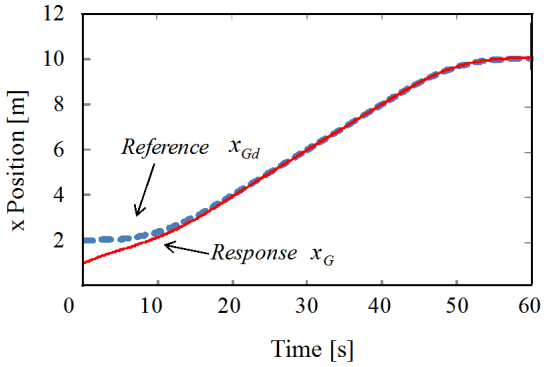

(a) Tracking performance for x position

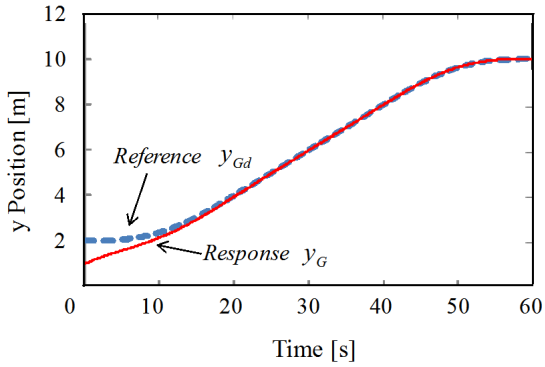

(b) Tracking performance for y position

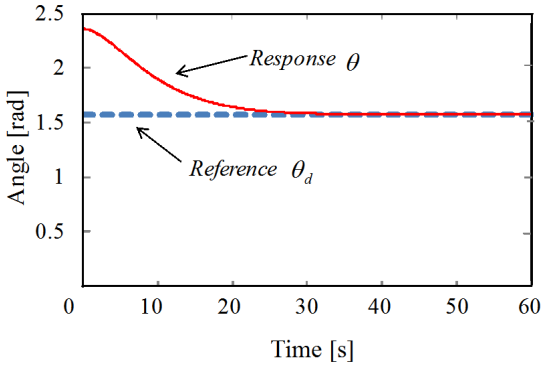

(c) Tracking performance for orientation angle θ

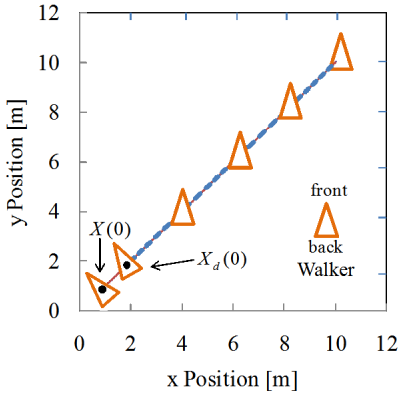

(d) Tracking and gradient of the walker

FIGURE 5. Simulation result of linear path with $m = 50$ kg and $r_0 = 0.20$ m

time after the start of the simulation (maximum 60 s), and the vertical axes indicate the x and y positions, respectively. Figures 4(c) and 5(c) show the tracking performance of the orientation angle. Figures 4(d) and 5(d) show the tracking and gradient of the omni-directional walker. In the figures, the dotted line represents the reference response and the solid line represents the adaptive control response.

For m= 0 kg and $r_0 = 0.00$ m, the walker can track the reference for both the x and y positions after 15 s, as shown in Figures 4(a) and 4(b), respectively. As shown in Figure 4(c), $\theta(0) = 2.36$ rad, and the reference response angle is set at $\theta_d(t) = 1.57$ rad. The orientation of the walker can align with the reference angle after 20 s. Finally, Figure 4(d), illustrating the tracking and gradient of the omni-directional walker in the working space, shows that the walker can successfully track a defined path with a constant orientation angle (i.e., a linear path) using the adaptive controller.

Figure 5 shows the simulation results for a linear path with $m = 50$ kg and $r_0 = 0.20$ m. In Figure 5(a), the x-position performance is similar to that shown in Figure 4(a). Similarly, the y-position response in Figure 5(b) resembles that in Figure 4(b). The simulation results in Figure 5(c) show that the walker can track a constant reference orientation angle as well as the case shown in Figure 4(c). Finally, the tracking and gradient results illustrated in Figure 5(d) shows that the adaptive controller can successfully track a linear path rapidly and accurately even with center-of-gravity shifts and load changes.

In order to thoroughly verify the adaptive method, the tracking performance for a circular path with a time-variant orientation angle (varying from 1.57 to 7.85 rad) was simulated and is shown in Figures 6 and 7. The trajectory described by (13) was used

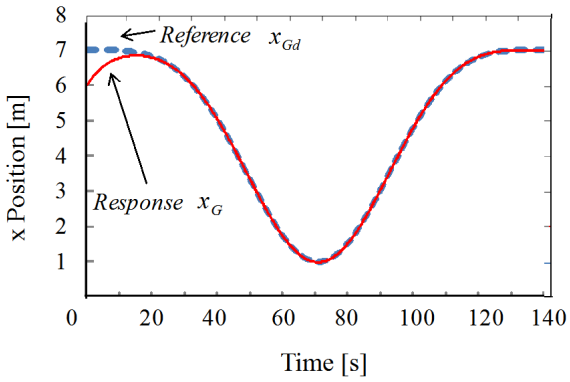

(a) Tracking performance for x position

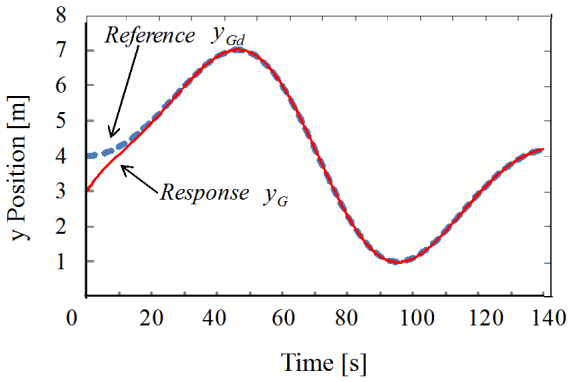

(b) Tracking performance for y position

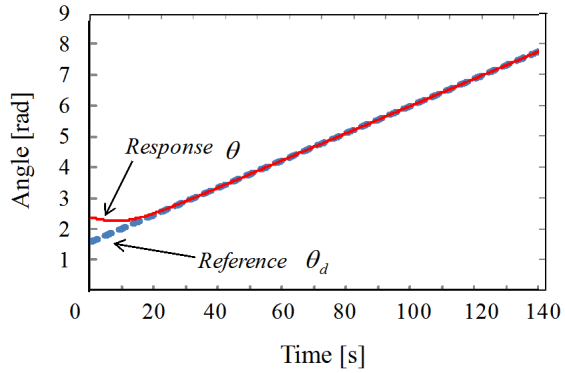

(c) Tracking performance for orientation angle θ

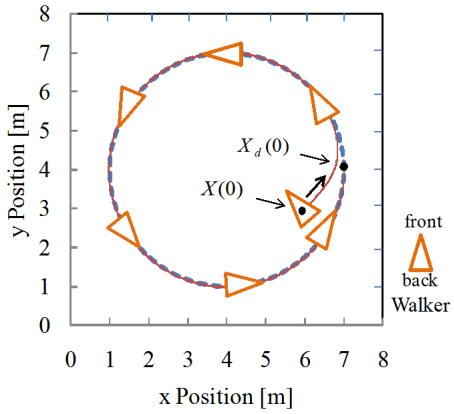

(d) Tracking and gradient of the walker

FIGURE 6. Simulation result of circular path with $m = 0$ kg and $r_0 = 0.00$ m

with initial positions $x_G(0) = 6$ m, $y_G(0) = 3$ m and $\theta(0) = 0.75\pi$ rad. The reference curve and adaptive control response are shown for 142 s.

Figure 6 shows simulation results for a circular path with $m = 0$ kg and $r_0 = 0.00$ m. The walker can track the reference target rapidly and accurately for the x position, y position, and time-variant orientation angle θ, as shown in Figures 6(a) – 6(c), respectively. The results for tracking and gradient are shown in Figure 6(d).

Figure 7 shows that the tracking performance of the omni-directional walker for a circular path and a time-variant orientation angle with $m = 50$ kg and $r_0 = 0.20$ m. The performance shown in Figures 7(a) – 7(c) is similar to that in Figures 6(a) – 6(c), even with the increase in mass from 0 kg to 50 kg and the shift of the center of gravity from 0.00 to 0.20 m. In the working space shown in Figure 7(d), both the tracking and gradient are almost identical to those in Figure 6(d).

To evaluate the path-tracking accuracy, path-tracking error E is defined as

$$E = \frac{\int_{x_s}^{x_e} |y_{Gd} - y_G| \, dx_G}{l} \tag{14}$$

where l is the length of reference path. Equation (14) calculates the area between the reference path and the response path and divides by l. In order to exclude the error caused by initial position deviation, the path-tracking error is calculated from 20 s to the end. The path-tracking error E for a linear path is calculated from $x_s = x_G(20)$ to $x_e = x_G(60)$ and circular path from $x_s = x_G(20)$ to $x_e = x_G(142)$. The path-tracking errors of the simulation are shown in Table 2.

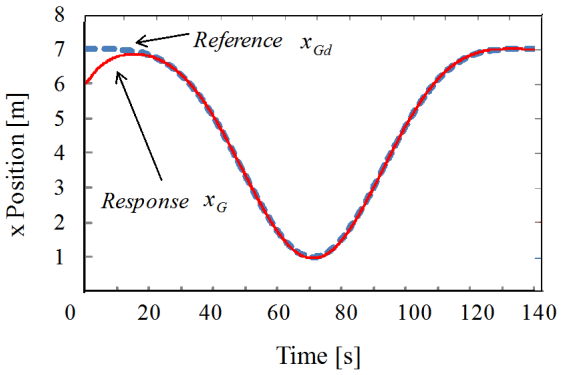

(a) Tracking performance for x position

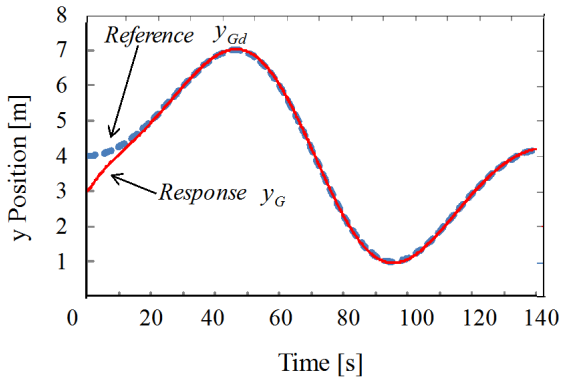

(b) Tracking performance for y position

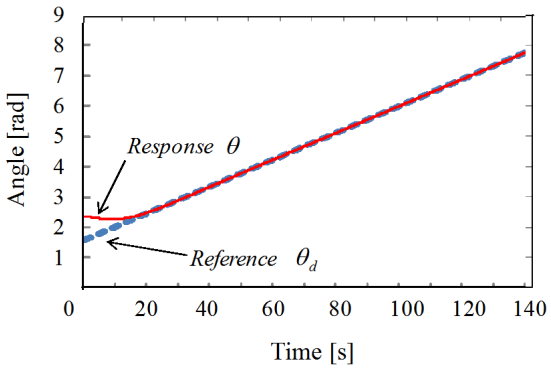

(c) Tracking performance for orientation angle θ

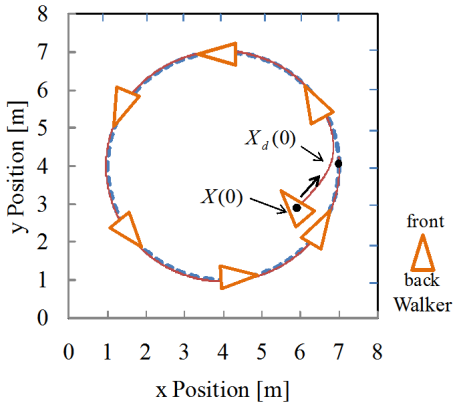

(d) Tracking and gradient of the walker

FIGURE 7. Simulation result of circular path with $m = 50$ kg and $r_0 = 0.20$ m

TABLE 2. Path-tracking errors

	Error (m)	
	$m = 0$ kg, $r_0 = 0.00$ m.	$m = 50$ kg, $r_0 = 0.20$ m.
Linear Path $x_s = x_G(20)$, $x_e = x_G(60)$	0.009	0.011
Circular Path $x_s = x_G(20)$, $x_e = x_G(142)$	0.008	0.014

As shown in Table 2, although the load changed from 0 to 50 kg and the center of gravity shifted from 0 to 0.20 m, the path-tracking error only increased by 0.002 m for a linear path. For a circular path, the path-tracking error only increased by 0.006 m. These data show the effectiveness of the proposed control method relative to that of the PID control described in [14].

Although only linear and circular paths are included in the simulation, the performance with respect to x position, y position, and orientation angle are all tested. The simulation results show that the proposed adaptive algorithm is feasible and effective for motion control that takes into consideration center-of-gravity shifts and load changes in the non-linear system of the omni-directional walker. These results also illustrate the advantages of the omni-wheels, which enable the walker to move in any direction while maintaining its orientation. Therefore, the omni-directional walker allows a more complex combination of motions in walking rehabilitation than other walkers.

The proposed adaptive controller can allow the controlled system converge to the global minimum point, which is different from the method in [15], which uses a potential function to avoid the local minima to compensate for the Lyapunov function. PI control with a compensator is effective for constant parameters, as shown in [16]. However, in this paper, the parameters (m or r_0) of the controlled system are time-varying, because of variations introduced by users, and the proposed adaptive controller can adapt to uncertainties and estimate the system parameter $\hat{\alpha}$ automatically. Therefore, the method is effective for this nonlinear system.

Matrix (B) in the proposed adaptive controller is based on the kinetic Equations (4). However, the kinetic equations cannot describe exactly the real walker because the walker is more complicated. Therefore, in the experiment, it is difficult to get the desired tracking performance only by adjusting the parameters. A method omitting matrix (B) will be proposed in future work.

5. **Conclusions.** In this paper, to reduce the error in path tracking of the omni-directional walker due to center-of-gravity shifts and load changes, an adaptive control algorithm was proposed for motion control of the walker. The simulation results demonstrate the effectiveness of the proposed algorithm. Therefore, the proposed adaptive control method is applicable for reducing path-tracking errors, showing its advantages for use in walking rehabilitation.

Future work will focus on further applying the proposed adaptive control algorithm to path tracking of the walker. Also, a method omitting matrix (B) will be proposed and its effectiveness in dealing with path-tracking errors will be tested in walking training.

Acknowledgment. This work is supported by Grants-in-Aid for Scientific Research Nos. 20240058 and 21300212 from the Japan Society for the Promotion of Science.

REFERENCES

[1] Y. Nemoto, S. Egawa, A. Koseki, S. Hattori, T. Ishii and M. Fujie, Power-assisted walking support system for elderly, *Proc. of the 20th Annual International Conference of IEEE Engineering in Medicine and Biology Society*, vol.5, pp.2693-2695, 1998.

[2] K. Kubo, T. Miyoshi and K. Terashima, Influence of lift walker for human walk and suggestion of walker device with power assistance, *International Symposium on Micro-NanoMechatronics and Human Science*, Nagoya, Japan, pp.525-528, 2009.

[3] H. Kobayashi, T. Karato and S. Nakayama, Emergence of gait by an active walker, *IEEE International Conf. on Robotics and Biomimetics*, Sanya, China, pp.1035-1040, 2007.

[4] S. Y. Wang, K. Kawata, K. Ishida, H. Yamamoto and T. Kimura, Omni-directional mobile walker for rehabilitation of walking, *The 17th Society of Life Support Technology*, 2001 (in Japanese).

[5] S. Y. Wang, K. Kawata, Y. Inoue, K. Ishida and T. Kimura, Omni-directional mobile walker for rehabilitation of walking which can prevent tipping over, *Japan Society of Mechanical Engineers Symposium on Welfare Engineering*, vol.39, pp.145-146, 2003.

[6] S. Y. Wang, H. Inoue, K. Kawata, Y. Inoue, M. Nagano, S. Ino, K. Ishida and T. Kimura, Developing the omni-directional mobile walker and verifying its effect of increase in the muscle power, *JSME Symposium on Welfare Engineering*, pp.176-177, 2007 (in Japanese).

[7] K. Ishida, S. Y. Wang, T. Nagano and T. Kishi, Development of an all-way mobile walker, *J. Physical Medicine*, vol.19, no.4, pp.246-250, 2008 (in Japanese).

[8] R. F. Stengel, *Optimal Control and Estimation*, Dover Publications, Inc., New York, 1994.

[9] P. Pannil, K. Tirasesth, P. Ukakimaparn and T. Trisuwannawat, Derivative state constrained optimal H2 control for unstable systems, *International Journal of Innovative Computing, Information and Control*, vol.5, no.10(B), pp.3541-3552, 2009.

[10] J. A. Shaw, *The PID Control Algorithm*, Process Control Solutions, New York, 2003.

[11] G. Tao, *Adaptive Control Design and Analysis*, University of Virginia, Charlottesville, 2003.

[12] D. N. Kouya and F. A. Okou, Adaptive backstepping control of a wheeled mobile robot, *The 17th Mediterranean Conf. on Control and Automation*, Thessaloniki, pp.85-91, 2009.

[13] J. J. Slotine and W. Li, *Applied Nonlinear Control*, Prentice Hall, Mill Valley, 1991.
[14] R. P. Tan, S. Y. Wang, Y. L. Jiang, K. Ishida and M. Nagano, Motion control of an omni-directional walker using adaptive control method, *ICIC Express Letters*, vol.4, no.6(A), pp.2189-2194, 2010.
[15] L. Jiang, M. Deng and A. Inoue, Obstacle avoidance and motion control of a two wheeled mobile robot using SVR technique, *International Journal of Innovative Computing, Information and Control*, vol.5, no.2, pp.253-262, 2009.
[16] S. Y. Wang, A new omnidirectional wheelchair and its motion control method, *ICIC Express Letters*, vol.4, no.1, pp.289-294, 2010.